# ON THE AIRBORNE SURVEY BY A HELICOPTER- A BRIEF OUTLINE AND SEVERAL ANALYSES OF THE SURVEY

Toshiyuki Tosha[1], Haruhiro Inagaki[2], Supri Soengkono[3] and Yoshiharu Kida[4]

[1]Inernational Research Organization for Advanced Science and Technology, Kumamoto University, 2-39-1 Kurokami, Chuo, Kumamoto 960-8555, Japan

[2]Geothermal Department, West Japan Engineering Consultants, Inc., 1-1-1 Watanabe-dori, Chuo, Fukuoka 810-0004, Japan

[3]GNS Science Wairakei, Private Bag 2000, Taupo 3352, New Zealand

[4] Geothermal Resource Development Department, Japan Oil, Gas and Metals National Corporation, 2-10-1 Toranomon, Minato, Tokyo 105-0001, Japan

tosha@kumamoto-u.ac.jp

**Keywords:** *Airborne survey, Gravity measurement, Spatial filter, Shape Index, Kuju geothermal field, Variogram, Fault structure*

## ABSTRACT

Heat discharge areas, where many geothermal features are found and high geothermal potential are expected, are often located in the mountain areas near volcanoes. It is hard to carry out ground explorations in these areas because of difficult access and high elevation changes. Moreover, the volcanic area is designated as a national park in many areas. Nearly 80% of the geothermal resources are presumed to exist in the natural parks.

Recently the deregulation of the geothermal development at Japanese national park was announced to encourage the development of geothermal energy for the energy security as well as combating global warning. With this announcement we are now able to develop geothermal resources at the lower category of the national park. Airborne geophysical survey is an effective method to acquire data from wide area without modification of the land surface. The survey using a helicopter has been conducted to obtain more scientific data for the exploration of geothermal prospects in the mountain regions near national parks.

Two kinds of surveys are organised. One is the survey using the gravity gradiometer, which measures partial gradients of the gravity, and the other is the magneto-electric measurement by the TEM (transient electromagnetic) method. We can expect to detect the fracture structure by the gravity gradient measurements and the extension of the conductive cap-rock by the TEM method over the geothermal fields. As of 1st June 2017, 12 areas have been surveyed by the airborne gravity gradiometer and 10 areas by the airborne TEM. In this paper we will show some results with spatial filter technique and a simple analytical method based on the theory of geostatistics to the gravity gradient data to reveal fracture and fault structures in the geothermal field

## 1.INTRODUCTION

Electric power generation by geothermal energy commenced operations in 1966 in Japan and the Matsukawa geothermal power plant celebrates its 50th anniversary in last year. The 8th October has been certificated on the anniversary for the geothermal development. In this year, 2017, the Otake power plant, the second geothermal power plant in Japan, will also celebrate its 50th anniversary. Electric generation using geothermal resources has had smooth growth for the first 30 years. The last large scale and conventional geothermal power plant was the Hachijo Geothermal Power Plant in 2000, with an installed capacity of 3.3 MW. No conventional geothermal power plant using steam has been constructed since then. The installed capacity of the geothermal power plants has been summed up to be about 515MW in Japan. However, the electricity generated by the geothermal resources only contributes to 0.2% of the whole electricity supply.

After the catastrophic earthquake and tsunami devastated the Pacific coast of north-eastern Japan on Friday, 11th March 2011, the Japanese government is encouraging the increase of the renewable energy supply including the geothermal. Increase of the renewable energy was originally decided against the global warming but after the disaster the percentage of the renewable energy was increased. There are, however, three major obstacles for geothermal development.

The development needs more a long time to construct the geothermal power plant. So much cost is necessary including interest. Adding the problem of the long lead time, high temperature fluid is mainly observed in the national parks and the high quality of the geothermal resources is limited. Hot springs are often found around the development area. However, financial support is conducted by JOGMEC (Japan Oil, Gas and Metals National Corporation) and Japanese government decided to introduced FIT (Feed In Tariff) for private company to make the development and the investment easily. Communication with local residents is encouraged, which is one of major discussion subjects in the joint workshop between GNS International and JOGMEC. Deregulations on the development in national parks and on the usage of the national forest are carried out and expected to permit a wider area for the development. A nation-wide survey is expected to review the potential of the geothermal resource in the national parks. JOGMEC conducts the airborne survey to cover wide area including the national parks. In this paper we aim to show several results of the airborne survey.

## 2. GEOTHERMAL DEVELOPMENT IN JAPAN

### 2.1 Global warming

By rapid increase of the fossil fuel use after the Industrial Revolution, Greenhouse gases (GHGs) such as carbon dioxide has increased, which caused environmental problems, the global warming. Mitigation against the global warming consists of several actions, which limit the long-

term human emission of GHGs in magnitude and in rate. The reduction of GHGs will be achieved by increasing the capacity of carbon sinks. One of the action is reforestation and another one is carbon sequestration, which captures carbon dioxide from the emission source and sink to the subsurface geological aquifer. Selection and usage of low carbon emission resource is also achieved to reduce GHGs. Mitigation policies can substantially reduce the risks of global warming with avoiding economy decay. Renewable energy is also expected to solve this most serious environmental problem in this century.

The Paris Agreement was adopted in COP21 (the 21st conference of the Party under The United Nations Climate Change Conferences) which aims to suppress GHG emission in order to hold the increase in the global average temperature to below 2 ˚C above pre-industrial levels. This agreement is a successor of the Kyoto Protocol, which is a previous guideline to reduce the emission in COP3. Geothermal energy has an advantage of low $CO_2$ emission.

The Paris Agreement requires Japan to reduce 26% of $CO_2$ emission against 2013FY (25.4% against 2005FY, 1,079 $MtCO_2eq$). Amount of reduction is greater than that in the Kyoto Protocol (6% against 1990FY). On the other hand, nuclear power generation became of less importance against the global warming after the serious accident of the nuclear power plant in 2011. Renewable energies become more of importance in generation of electricity. Geothermal energy as well as other renewable energies has advantage in their low $CO_2$ emission.

### 2.2 The Long-term Energy Supply and Demand Outlook

After the terrible Fukushima disaster happened in March, 2011, demand for stable and renewable energy supply has been increasing. METI approved and announced " The Long-term Energy Supply and Demand Outlook" on 16 July 2015 pursuant to the policies of the Strategic Energy Plan, which includes the electricity generation mix (Energy Mix) to 2030. Nuclear power generation is set at 20% to 22%, renewables at 22% to 24%, coal at 26% and LNG at 27% of total electricity supply in 2030. In 2030 $CO_2$ emissions would be 21.9% lower than in 2013, and the primary energy self-sufficiency rate would increase from 6.3% in 2012 to 24.3%. On the basis of this political decision geothermal is expected at 1.0 to 1.1% of total generation, which is about three times at present (Figure 1).

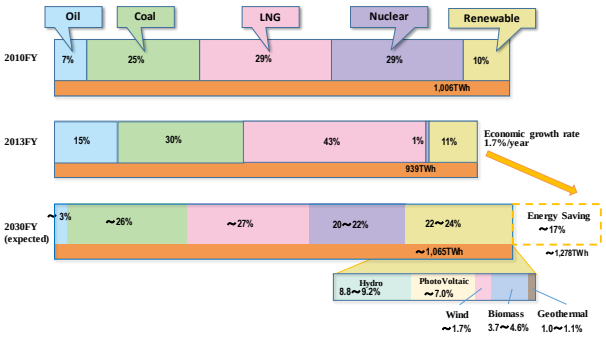


**Figure 1: Electricity generation in 2030 (Energy Mix)**

### 2.3 Deregulation on the development

Three ministries are relevant organisations for geothermal development; the Ministry of Environment (MOE), the Ministry of Agriculture, Forestry & Fisheries (MAFF), and the Ministry of Economy, Trade & Industry (METI).

The National Conservation Bureau of MOE is a regulatory agency from the point of the view of the conservation of the national parks, though the Global Environment Bureau of MOE is encouraging the use of geothermal energy for the reduction of $CO_2$ emissions. The deregulation has been made recently so that geothermal development in national parks will be permitted under some conditions, while still preserving the environment. MAFF gives permission for the use of the national forests as many geothermal fields are located in the national forests. Deregulation to the MAFF on the usage of the national forest is also expected to permit a wider area to use for development.

The geothermal development needs more than 10 years to construct the power plant with more than 10MW capacity since the commencement of the development. The deregulation to shorten the development time is also requested. There is an attempt to use simulation to judge the environmental impact.

### 2.4 Communication with local residents

Onsen (Hot Spring) owners are wary about the depression of their hot spring resource and some of them have strong opinion against the geothermal development. In the past there was wrong explanation for the onsen owners that geothermal resources locate much deeper than hot spring resource and there is no damage to hot spring resource by the development. Careful monitoring is necessary to watch the damage of hot spring resource. Moreover, the communication is the most important to build a good relationship between the developer and local residents including the hot spring owners. Several local governments enacted ordinances for the development and launched a committee to discuss geothermal development.

### 2.5 Financial support

The committee in the Japanese Government reported that it takes about 25.9 billion JPY (Approx. 330 million NZD) to construct a 30MW Geothermal Power Plant (Cabinet office, 2011). The construction of the power plant house and the installation of the turbine and generator need huge costs. Huge costs are also incurred in the exploration part of geothermal resource development. Even if a promising geothermal reserve is found at the exploration stage, major risks still remain, such as necessity of the long period between completing the construction of a power station and its being brought on stream. The development of the geothermal field and the construction of the power plant are conducted by different companies in Japan, which is one of the reasons why the development is so slow. Electric power company takes a roll to construct power plant and requests to steam production company to show enough steam to operate. The report also pointed out the long development time, which is estimated to be more than 11 years to complete a 30MW Geothermal Power Plant project from start to finish (Cabinet office, 2011). To cope with these risks, JOGMEC offers several types of financial support, including subsidy, equity capital, and liability guarantee. For example, subsidies will be applied for a survey period, equity capital

for an exploration period and liability guarantee for a construction period of the power plant for the development in Japan.

## 3. AIRBORNE SURVEY

### 3.1 National wide geothermal survey

A nation-wide geothermal survey is widely required by both developers and researchers. The promoting survey projects conducted by NEDO (New Energy Development Organization, currently New Energy and Industrial Science Development Organization) had investigated more than 60 geothermal fields in Japan and five geothermal power plants commenced in operation. The new geothermal power plant (tentatively named the Wasabizawa Power Plant) is being constructed at the surveyed area in Yuzawa City and will start in 2019. The nation-wide survey is very important to supply fundamental data for the geothermal development. After the deregulation geothermal development in national parks has been permitted under some conditions. A new nation-wide survey is requested.

The geothermal fields in Japan are mostly associated with Quaternary volcanoes and distributed in mountainous areas or within national parks, where it is difficult to access and to investigate. Nearly 80% of the geothermal resources are presumed to exist in the natural parks. Airborne geophysical survey is an effective method to acquire data from wide area without modification of the land surface and also a useful technique to explore Japanese geothermal fields. The survey using a helicopter has an advantage to cover maintain area including national parks.

### 3.2 Survey plan

Airborne geophysical surveys are conducted which aim to acquire basic data for the evaluation of geothermal resources in order to promote geothermal development. There are two survey methods are selected using a helicopter. The survey is planned to be conducted all over Japan, especially in the Kyushu, Tohoku, and Hokkaido regions, where many geothermal power plants are located and installed. Some of the national parks are located near volcanoes and geothermal resources are associated with the volcanoes. One is gravity and the other is resistivity surveys.

The airborne gravity in our system uses a gravity gradiometer, which measures the spatial variation of the gravitational acceleration, implying that the gravity is measurable with high resolution compared to the conventional gravity survey. The gradiometer measures the gravity tensor though the conventional gravity meter measures only the vertical component of the gravity vector. A time domain electromagnetic survey to provide an extensive resistivity structure around geothermal fields. The outline of the survey and the history of a national-wide survey in Japan were reported in the workshop (Tosha et al., 2015).

## 4. ANALYSIS METHOD

### 4.1 Spatial filter

#### 4.1.1 HGA (Horizontal Gradient Analysis)

There are many methods to analyse the gravity gradient tensor (spatial second derivative of gravity potential), a simple way is to display the secondary vertical differential (Gzz) because the subsurface anomalies mainly effect the vertical components of the gravity potential. Therefore it is reasonable to display Gzz, the vertical derivation of Gz. The subsurface anomalies also affect the horizontal change of the gravity vector. It is also reasonable to display the horizontal component of the gravity tensor such as Gxz, Gyz and so on.

HGA is a technique for quantitatively knowing the rate of change of gravitational anomaly in the horizontal direction and is often used for detecting sudden change zone of gravity anomalies due to structural change such as fault (e.g. ten Brink et al., 1993). HGA of gravitational anomaly is given by the following equation, assuming that the gravity abnormal value is Gz.

$$HGA = \sqrt{\left(\frac{\partial G_z}{\partial x}\right)^2 + \left(\frac{\partial G_z}{\partial y}\right)^2}$$

#### 4.1.2 TDR (Tilt Derivative)

There is another method to identify the geological structure of normalizing the gradient by the gradient in another direction. Miller and Singh (1994) proposed TDR (Tilt Derivative), which is an arc tangent of the normalized value of the vertical first derivative (Gzz) by the horizontal differential (HGA) of Gz.

TDR is effective for detecting both shallow and deep structures, and the position where it is 0 indicates the boundary of the structure.

$$\mathrm{TDR} = \arctan\left[\frac{\frac{\partial G_z}{\partial z}}{\sqrt{\left(\frac{\partial G_z}{\partial x}\right)^2 + \left(\frac{\partial G_z}{\partial y}\right)^2}}\right]$$

TDR is known as a balanced filter or semi-automatic interpretation method which does not detect a short wavelength anomaly with extremely large amplitude. However, when positive and negative gravity anomalies are adjacent TDR shows a structural boundary which does not actually exist (Cooper and Cowan, 2006; Ma, 2013).

The underground structure change happens not only in the vertical direction but also in the horizontal direction. A method to normalize the gravitational gradient in one direction with that in another direction can avoid extreme amplitude and is a well-balanced method. TDR had a major impact on the development of semi-automatic interpretation method (JOGMEC, 2015).

#### 4.1.3 SI (Shape Index)

When a high-density abnormal body exists in shallow subsurface, the gravity is affected by the high density abnormal body. An equal gravity potential plane shows a convex shape above the high density body. In order to make the geological boundary clearer than Gzz and make it easier to interpret geological structure, Shape Index (SI) representing the shape of the equal gravity potential plane has been proposed (Koenderink and can Doom, 1992; Roberts, 2001; Cevallos et al., 2013). SI is attended to focus on the curvature of the potential surface such as gravity.

$$SI = \frac{2}{\pi} arctan\left[\frac{\frac{\partial G_z}{\partial z}}{\sqrt{\left(\frac{\partial G_x}{\partial x} - \frac{\partial G_y}{\partial y}\right)^2 + 4\left(\frac{\partial G_x}{\partial y}\right)}}\right]$$

SI takes values from -1 to 1. SI becomes 1(Dome) when the gravity potential plane is bulging upward, 0(Flat) when it is flat, and -1 (Bowl) in the shape of a bowl dropping downward. As the SI decreases, the shape of the potential plane changes from Dome, Ridge, Flat, Valley to Bowl. Since the SI is positive and negative in the case of positive and negative gravity anomaly, respectively, it is possible to process the shape of the gravity basement numerically.

### 4.2 Variogram

#### 4.2.1 Definition of variogram

Variogram is a statistical method that characterizes the spatial continuity or roughness of a data set and was developed to estimate the quality of gold at gold mines (e.g. Davis, 1973). As the variogram is characterized to notate spatial features, it is not limited to use in mines, but in meteorology and agricultures. Variogram is often used as a geostatistics method with geological and geophysical data.

In the case of two data sets, the continuity of the space may be quite different even if the one-dimensional analysis of the variogram is almost identical. Variogram consists of the experimental variogram calculated from the data and the variogram model fitted to the data.

An experimental variogram (γ) is calculated sum of the square of the difference between observed values (Zi and Zj) at two observation sites (i and j) to all pairs where the geographical distance between two sites is equal to or less than a certain value (h) and is divided by a number of pairs (N) and a factor of two as follows;

$$\gamma(h) = \frac{1}{2|N(h)|}\sum_{N(h)}(Z_i - Z_j)^2$$

γ (h)is exactly called a semi-variogram, and the variogram is called the value 2 γ (h) before dividing by a factor of two, but in many cases both definitions are confused. In this paper we call γ (h) as a variogram. In addition, two observed sites (i and j) are distributed in a space then the variogram can be generally regarded as a vector. We will treat the variogram as a scalar value because the paired data were obtained from the observation result when the helicopter flew to one straight line.

N (h) is the number of observation pairs whose distance is h, but when the distance is within the range of allowable error (± Δh), the distance is assumed to be h. The calculation result is called an experimental variogram.

| | |
|---|---|
| Count | 10251 10251 |
| Average | 100.00 100.00 |
| Standard Deviation | 24.11 24.11 |
| Median | 100.35 100.92 |
| 10 Percentile | 73.98 73.95 |
| 90 Percentile | 125.91 124.72 |

**Table 1: Some common statistics of two data sets**

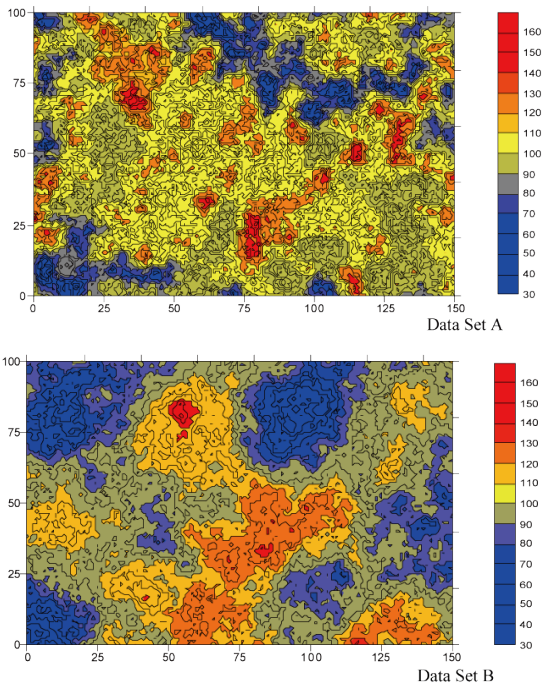


**Figure 2: Two synthetic data set for variogram analyses**

Since the experimental variogram γ (h) is discrete, it is hard to use, so we approximate the experimental variogram with continuous function, which is called a variogram model. A variogram model is selected from one of the best fitted function to the experimental variogram such as spherical, exponential, and linear In this study we calculate the experimental variogram from the data taken by the helicopter.

#### 4.2.2 An example of variogram

There is an example of variogram (Golden Software, http://www.goldensoftware.com/VariogramTutorial,pdf) by the base of two synthetic data sets with similar statistics such as count, average, standard deviation and so on. There is no difference between the statistical distribution and the histogram between two groups, but the original data are shown in Figure 2.

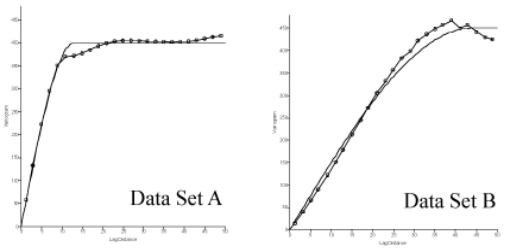


**Figure 3: Experimental variograms with variogram models (solid lines) for two synthetic data sets**

Data set A and data set B show a completely different spatial distribution. A particularly noteworthy feature is that rapid changes in space are predominant, and high value zones (red patches) and low value zones (blue patches) are intermingled in dataset A. On the other hand, high value zones and low zones spatially continue in data set B. Although there is a

clear difference in the spatial distribution, there is small statistical difference between the two data sets in the mean value, the variance, the histogram, etc. because the position information is lost.

Variogram can characterise the continuity (or roughness) of the space of a data set which is basically expressed in a two-dimensional graph. Figure 3 shows variogram for these two data sets. The initial slope difference of the curve is obvious. Since the variogram contains space information, it is used as a method of estimating the missing value at the interpolation and an isogram such as an isothermal plot will be made. The kriging is used a variogram model estimated from experimental variogram and is the most commonly used as this interpolation method.

### 4.2.3 Application to gravity survey data

If we assume that the total number of the data set (N) is sufficiently larger variogram can be expressed by unbiased estimate of population variance(V), the autocovariance (C), the autocorrelation coefficient(r) as follows (Shoji and Koike, 2007);

$$\gamma(\mathrm{h}) = V - C(h)$$

$$= V\{1 - r(h)\}$$

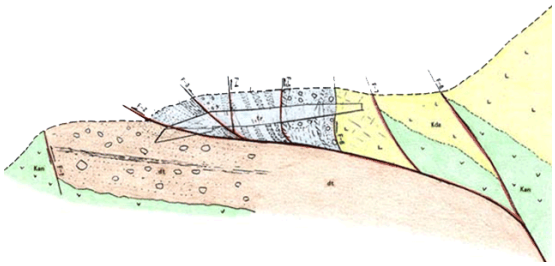

**Figure 4: A schematic model of flower structure**

This relationship suggests that the autocorrelation becomes high at a certain distance h and then the variogram becomes zero. Since the variogram is one of representations of autocorrelation, it is expected that the variogram takes a minimum value if any geological event or feature are repeated. The flower structure is often generated at the surface when the fault generates (Woodcock and Fisher, 1986). If the faults have equal intervals, there is a possibility that the flower structure make minimum values in variogram.

## 5. KUJU GEOTHERMAL FIELD

### 5.1 Geological setting

Central-Kyushu is known as a volcano-tectonic depression region formed under a tensile stress field after the Neogene time. The Beppu-Shimabara graben is characterized by low gravity anomalies, which extends from the Beppu Bay to the westward. Kuju geothermal field is located in the southeast part of the graben as shown in Figure 5 (after Fujita and Abe, 1988).

In this graben there are uplifting zones of Kuju, Moizuwake-toge, Garandake-Yuyama, and Asono. There are also subsiding zones of Shishimuta, Shonai, Beppu, Oita and Kuju(another local place as same name as the uplifting zone). The Kuju uplifting zone has a trapezoidal shape from a topographical view point, and the northeast margin of this

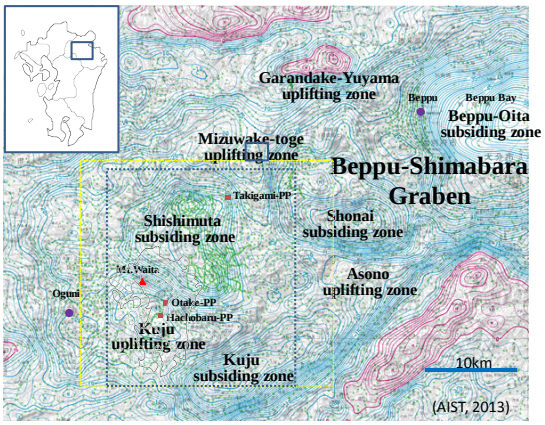


**Figure 5: Subsiding and uplifting areas on the Bouguer anomaly map. Broken lines show the boundaries of the area for the filter and the variogram analyses.**

uplifting zone forms steep slope, which contacts to the Shishimuta subsiding zone. Fractures with faults in northwest-southeast direction associated with geothermal resources are expected in the steep slope. Other fractures in northeast-southwest direction intersect orthogonally to the previous fractures near Sugawara, and geothermal resources with high permeability have been developed. Lineament has also developed in northwest-southeast and northeast-southwest directions. Shishimuta subsiding zone is originated of a caldera that was active from about 1Ma to 900ka, and this caldera spurted a large amount of pyroclastic flow (Gyagyo pyroclastic flow and Imaichi pyroclastic flow) by two large eruptions. Geothermal systems are expected in the steep slopes around subsiding zone, and the Hohi geothermal area located around Shishimuta subsiding zone is regarded as a typical geothermal field in Japan.

### 5.2 Survey Area

The area shown as broken lines in Figure 5 shows the extent of the airborne exploration in Kujyu area (JOGMEC, 2016). The survey area is approximately 20 km in east-west, 25 km in north-south. The helicopter flew at a line in the north-

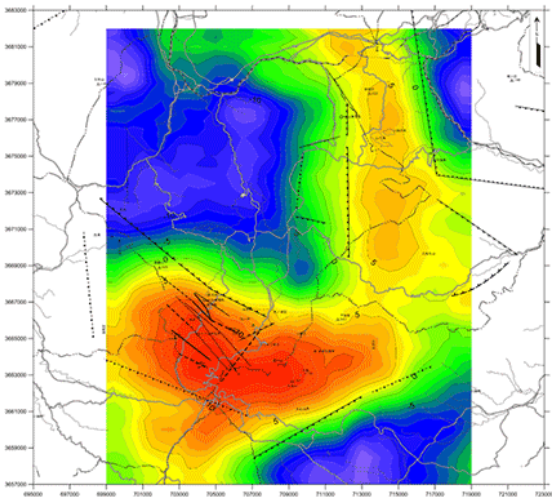

**Figure 6: Gravity (Gz) map on the survey area**

south direction with an interval of 250 m. Since the Otake and the Hachibaru geothermal power plants are located in the Kokonoe uplifting zone, a detailed survey were conducted with a line interval of 125 m around the geothermal plants. The survey took place from 10 October to 28 October 2014 of about 20 days. For the detailed area it took about 7 days.

## 6. DISCUSSIONS

### 6.1 Filter analysis

Figure 6 shows the distribution of the vertical component of gravity Gz. Surface gravity surveys also made a map as the same as the figure (Komazawa and Kamata, 1985). In this map, the high and low gravity anomaly zones are roughly in agreement with the uplifting and the subsiding areas estimated from the gravity analysis. The low gravity anomaly zone is called the Shishimuta subsiding zone, which was made by the subsidence of the caldera, and the gravitational change happen inside of the geothermal areas, where Hatchobaru, Otake, and Takigami power plants, Sugawara binary power station and Hosenji hot spring are located.

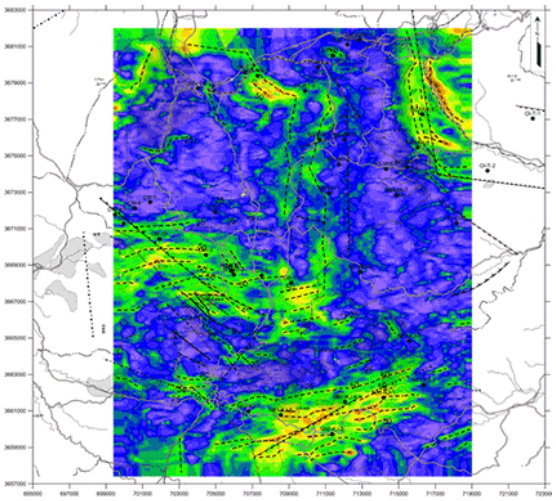

**Figure 7: Map after HGA filter is applied**

Figure 7 shows a map analysed by the HGA method, which is suitable for detecting abrupt change of gravity and is frequently used to extract discrepancy of the subsurface structure. The black dashed lines in the figure indicate the line structure extracted by the HGA. In this figure, the maximum values continue to the edge of the Shishimuta subsiding zone and are especially distributed around the boundaries of the subsiding zone and the Mizuwake-toge and the Kuju uplifting zones. This implies that the distribution of maximum values shows a sudden change in gravity basement depth at the edge of Shishimuta subsiding zone. The maximum values are also observed near the fault structure extending roughly in the directions of north-northwest and south-southeast and northeast-southwest, which was reported and presumed at the eastern margin of the Mizuwake-toge uplifting zone and the southern margin of the Kuju uplifting zone by Komazawa and Kamata (1985).

Figure 8 shows the distribution map of TDX (normalized horizontal tilt angle), an advanced spatial filter. TDX is a

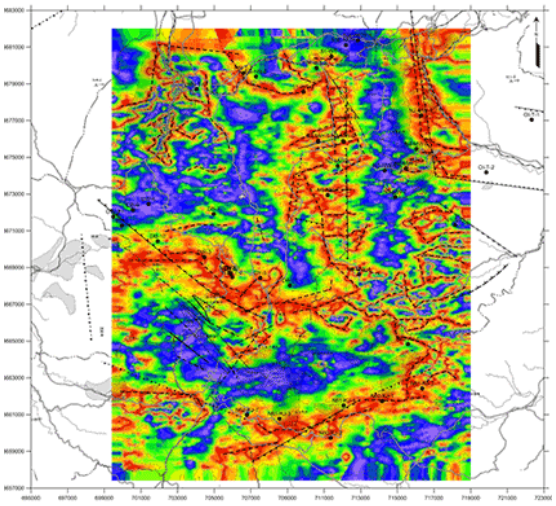

**Figure 8: Map after TDX filter is applied**

filter showing the maximum value around the place with the sudden change of gravity (JOGMEC, 2016). Although the figure shows a slightly complicated distribution, maximum values of TDX are distributed in the margin of the Shishimuta subsiding zone, the eastern margin of the Mizuwake-toge uplifting, and southern margin of the Kuju uplifting as the same as the HGA map. The TDX maximum values indicate the gravitational abrupt change accompanying a sharp depth change of the gravity basement.

In addition to the north-south line structure in the western margin of the Mizuwake-toge, another line structure which is extending roughly east-northeast and west-southwest direction was extracted. Other line structures were not extracted by HGA but are extracted by TDX in northwest and east regions in the investigation area. They show possibly geographical structures such as faults. TDX has, however, been confirmed to be a powerful high-pass filter, and there is a high possibility of extracting line structures that do not actually exist. Therefore, it is necessary to confirm the line structure with reference to consistency with another filter analysis and the geological map showing known faults.

Figure 9 shows the Shape Index (SI) distribution map. SI has a value in the range of -1 to 1. As a guide of the structure, + 1 is corresponded to Dome, + 0.5 to Ridge, 0 to Flat, -0.5 to Valley, -1 to Bowl structures.

There are high SI regions with the value near 1 in the Kuju uplifting, which locate in the southwestern and southern part of the survey area, and in the Mizuwake-toge uplifting distributed in the northeastern area, suggesting the shallow and dome structure of the gravity basement. On the other hand, the low SIs, which are roughly distributed from the central to northwest survey area, agree with the expansion of the Shishimuta subsiding zone, indicating the depression and bowl structure of the gravity basement. SI values of -0.5 and 0.5 might show the place where the depth of the gravity basement is suddenly changed. In Figure 9 contour lines with SI of -0.5 and 0.5 are drawn in an emphasized colour to help to extract the line structure associated with geothermal resources. The line structure based on SI is slightly different from those analysed by SHA and TDX analyses and they extend generally in the north-south and the northwest-southeast direction in the Kuju uplifting zone and roughly from the east-west to east-northeast and west-southwest directions.

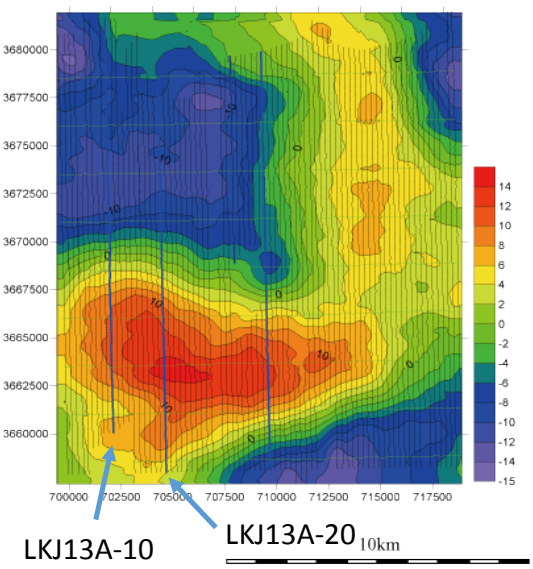


**Figure 10: Airborne survey lines on the map of Gz**

### 6.2 Variogram analysis

As pointed out in the previous chapter, five components of the gravity tensor are independent. However, AGG measures two components. In order to complete tensor components compensation algorism is necessary based on Fourier transform and/or Equal potential methods. Moreover, AGG measures about 3m interval along the flight but flight line interval is about 250m. Filter analyses assume homogeneous 2-dimensional data but AGG is far away from the homogeneity. Therefore, we tried to clarify fault by the variogram as a method to analyse only from actual measurement data.

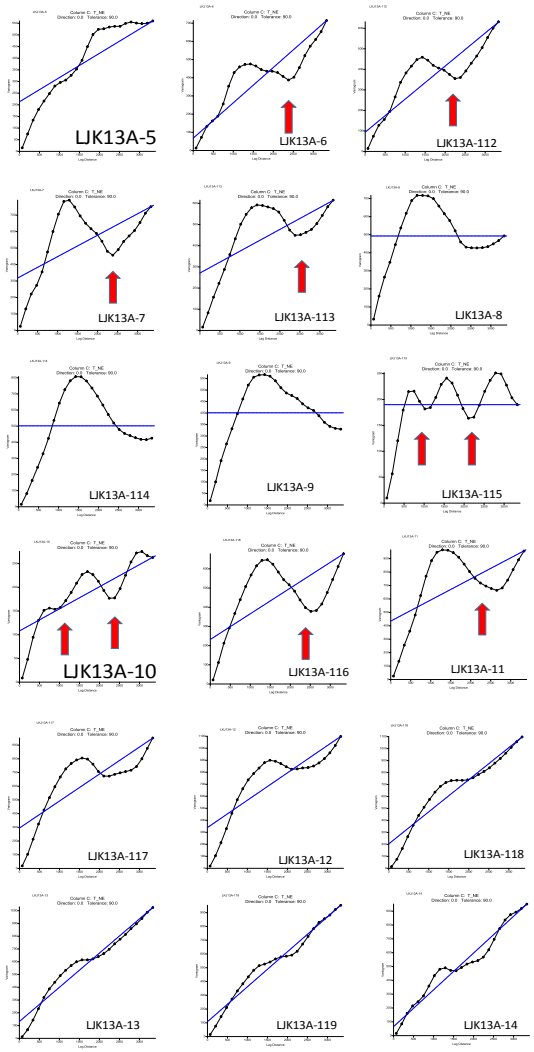


**Figure 11: variograms used all data along the survey line from west to east.**

The survey lines used in the variogram analysis are shown in Figure 10 with example of the survey line names such as LKJ13A-10 on the distribution map of the vertical

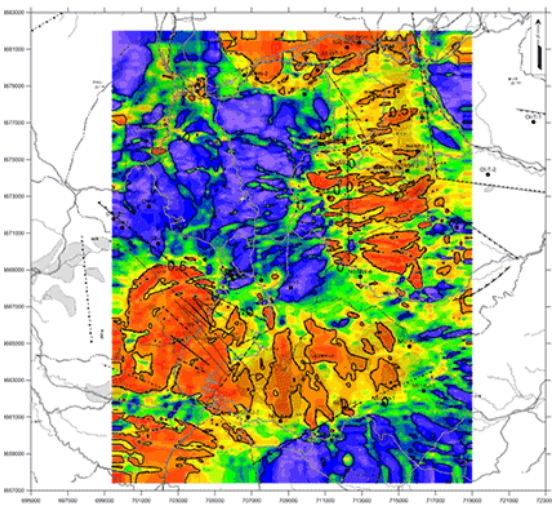

**Figure 9: Map after SI filter is applied**

component of gravity Gz (the same figure as Figure 6). For each survey line data, the variogram was calculated. An example of variogram along a survey line is shown in Figure 11. The minimum value of the variogram is indicated by a red allow. Each variogram shows the result of the analysis along each survey line from west to east. Analyses showed that the survey lines which have the local minimum in the variogram plot are not scattered but relatively localized. In other words, it is estimated that the fault does not appear in all the survey lines, but rather in a relatively coherent position. It is possible to estimate the interval when the faults are equally spaced but it is impossible to know in which part of the survey line the faults exist. In order to estimate the

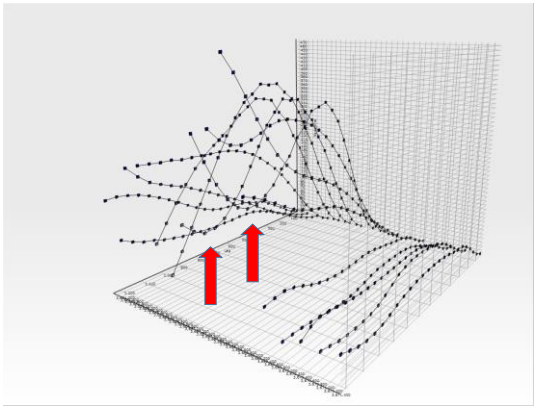

**Figure 13: A computer program and display to show variograms**

location of the fault, we used a partial data set in a certain section instead of using all station data. By shifting the section, it will be possible to estimate where the fault develops much.

It is too hard to determine the minimum value of variogram with a small number of the data set. On the other hand, many data conceal the minimum values. We changed the number of points used to calculate the variogram to find out the optimum number of data. The number of measurement points of 2,500 (about 7.5 km length) is a suitable length for the analysis to extract the fault structure. Based on this result, We moved the analysis start point by 500 points at an interval of 2500 points along the survey line (LJK13A-10). The result is shown in Figure 12 implying that faults are developed around 3000 points (about 9 km from north end of the survey line) and 3500 points (about 10.5 km). Around the analysed point fault systems develop in the gravity. Around the analysed point fault systems develop in the gravity map in Figure 6. It might be possible to estimate the area where the fault develops using variograms.

## . CONCLUSION

HGA, TDX and SI filters were applied to six components of gravity gradient tensor acquired by AGG exploration by a helicopter. As a result of these filter analyses, many line

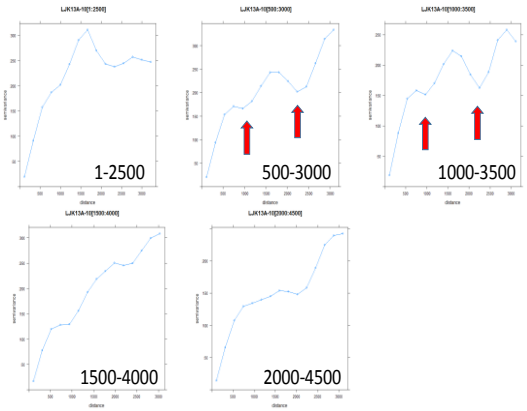


**Figure 12: Variograms with various start point in a fixed interval of 2500 points**

structures that may indicate faults were detected in marginal area of the Shishimuta subsiding zone, the Kuju and the Mizuwake-toge uplifting zones. Since there are many geothermal power plants located in the margin of the Shishimuta subsiding zone, the line structures possibly indicate the geological structure which regulates the flow of the geothermal fluid.

Variogram is effective as one analysis method with simple calculation. There are, however, drawbacks such as the inability to locate the fault position. Since airborne geophysical survey aims to perform investigation as a preliminary stage of precise survey, variogram is possibly suitable, which achieves the approximate existence range of the fault. We have made a computer program that specifies the cutout width from one survey line and displays the experimental variograms while shifting the starting point. Figure 13 shows an example of the result of the survey line (LJK13A-10). It can be seen that there are two experimental variograms taking the minimal values, suggesting the fault structures.

## ACKNOWLEDGEMENTS

The authors would like to express their deep gratitude to the management of JOGMEC survey project. The authors would like to thank great cooperation of various related parties of local governments, Fugro Japan Co. Ltd., Nakanihon Air Service Co. Ltd. to support the survey. The authors also thank Dr. Akihiko Chiba of Sumiko Resources Exploration & Development Co. Ltd. and Dr. Koichiro Fukuoka of Kyushu Geophysics Co. Ltd. for their help to analyse and to discuss the results.

## REFERENCES

AIST (National Institute of Advanced Industrial Science and Technology) : Gravity database of Japan, DVD edition, (2013).

Cevallos, C., Kovac, P. and Lowe, S. : Application of curvatures to airborne gravity gradient data in oil exploration, Geophysics, 78, 4, G81, (2013).

Cooper, G. R. J., and Cowan, D. R. : Enhancing potential field data using filters based on the local phase, Comp. Geosci., 32, 1585, (2006).

Davis, L.C.: Statistical and data analysis in geology, John Wiley & Sons, Inc., New York, 550, (1973).

Fujita, T. and Abe, M.: Survey of Oguni geothermal field, Kyushu district, Japan, Chinetu(Geothermal), 25, 4, (1988) (in Japanese with English abstract).

JOGMEC: Report to examine methods for using airborne survey data of gravity measurement, 246,(2015) (in Japanese).

JOGMEC: Report Geothermal resource evaluation work of "Kuju area" based on gravity deviation data (Phase 1)-Filter analysis and evaluation work, 50, (2016) (in Japanese).

Koenderink, J. J., and van Doornm A. J. : Surface shape and curvature scales, Im. Vis. Comp., 10, 5557. (1992).

Komazawa, M. and Kamata, H.: The basement structure of the Hohi geothermal area obtained by gravimentric analysis in central-north Kyushu, Japan, Rept. Geol. Surv. Japan, 264, 303, (1985) (in Japanese with English abstract).

Woodcock, N. H. and Fisher, M. : Strike-slip duplexes Jour. Struct. Geol., 8, 725, (1986).

Ma, G. : Edge detection of potential field data using improved local phase filter, Expl. Geophys., 44, 36, (2013) .

Miller, H. G., and Singh, V. : Potential field tilt – A new concept for location of potential field sources, Jour. Appl. Geophys., 32, 213, (1994).

Roberts, A. : Curvature attributes and their application to 3D interpreted horizons, First Break, 19, 85, (2001).

Shoji, T. and Koike, K.: Variogram-Data analysis of spatial continuity, J. Geotherm. Res. Soc. Japan, 29, 125, (2007) (in Japanese with English abstract).

ten Brink, U. S., Ben-Avarham, Z., Bell, R. E., Hassouneh, M., Coleman, D. F., Andreasen, F., Tibor, G., and Coakley, B. : Structure of the Dead Sea Pull-apart Basin from Gravity Analyses, J. Geophys. Res., 98, 21877, (1993).

Tosha, T., Shimada, T., and Fukuda, M: Data analyses of the airborne survey to clarify the geothermal structure and to evaluate the geothermal potential, Proc. NZGW, 136, (2015)